Supporting Information

Novel multi-functional sites in boron-based bi-atom catalysts synergistically boost C-C coupling for efficient CO electroreduction towards ethanol

*Huong T. D. Bui and Tore Brinck**

Department of Chemistry, CBH, KTH Royal Institute of Technology, SE-100 44 Stockholm, Sweden

*To whom correspondence should be addressed. E-mail: tore@kth.se

Computational Methods

The computational hydrogen electrode model (CHE)[1] was employed to calculate Gibbs free energy (ΔG) change of each elementary reactions via $\Delta G = \Delta E + \Delta E_{ZPE} - T\Delta S + \Delta G_U + \Delta G_{pH}$ where ΔE, ΔE_{ZPE}, and ΔS denote the electronic energy difference, the zero-point energy change and the entropy change. Zero-point energy was obtained from the vibrational frequencies via the equation: $E_{ZPE} = \sum_i hv_i/2$, and entropy was calculated using the following equation: $S = k_B T \sum_i^{3N} [-\ln\left(1 - e^{-\frac{\varepsilon_i}{k_B T}}\right) + \frac{\varepsilon_i}{k_B T\left(1-e^{\frac{\varepsilon_i}{k_B T}}\right)}]$ where ε_i is the vibrational energy of mode i, N is the number of atoms in the adsorbates, k_B is Boltzmann constant (1.38 x 10^{-23} JK^{-1}),T = 298.15 K. ΔG_U is the free energy contribution related to electrode potential U, as expressed via $\Delta G_U = -eU$ (e and U are the number of transferred electrons and applied electrode potential, respectively). ΔG_{pH} is the free energy correction of pH, $\Delta G_{pH} = 0$ for acidic medium in this work. The entropies of free gas molecules were taken from the National Institute of Standards and Technology (NIST) database. The limiting potential (U_L) of the reaction was calculated as $U_L = -\Delta G_{max}/e$, where ΔG_{max} is the free energy change of potential determining step and e is the corresponding number of electrons transferred. Average adsorption energy of CO* co-adsorbed species is calculated as avg_E_{ads}[2CO*] = ($E_{2CO*\text{-}BACs} - E_{BACs} - 2*E_{CO(gas)}$)/2, where $E_{2CO*\text{-}BACs}$, E_{BACs} and $*E_{CO(gas)}$ are total energies of 2CO*-adsorbed BACs, bare BACs and CO gas phase.

The formation energy of B-X bi-dopants into silicene (B-X@Si) is calculated as: $E_f = E_{BACs} - E_{DV-Si} - E_{B\ dopant(bulk)} - E_{X\ dopant(bulk)}$, where E_{BACs}, E_{DV-Si}, $E_{B\ dopant(bulk)}$ and $E_{X\ dopant(bulk)}$ are the total energies of BACs, di-vacancy (DV) silicene, and single B and transition metal (TM) dopant in bulk state. The electrochemical stability of transition metals in B-doped silicene (B@Si) can be evaluated by the dissolution potential (U_{diss}),[2] which is defined

as $U_{diss} = U^{o}_{diss} - E_f/Ne$, where U^{o}_{diss}, E_f and N are the standard dissolution potential of pure bulk, formation energy ($E_f = E_{BACs} - E_{SV-B@Si} - E_{TM\ dopant(bulk)}$; E_{BACs}, $E_{SV-B@Si}$ and $E_{TM\ dopant(bulk)}$ are the total energies of BACs, single vacancy (SV) B@Si, and single transition metal dopant in bulk state, respectively), and the number of electrons involved in the dissolution. Hereby, materials with U_{diss} > 0 V are considered electrochemically stable.

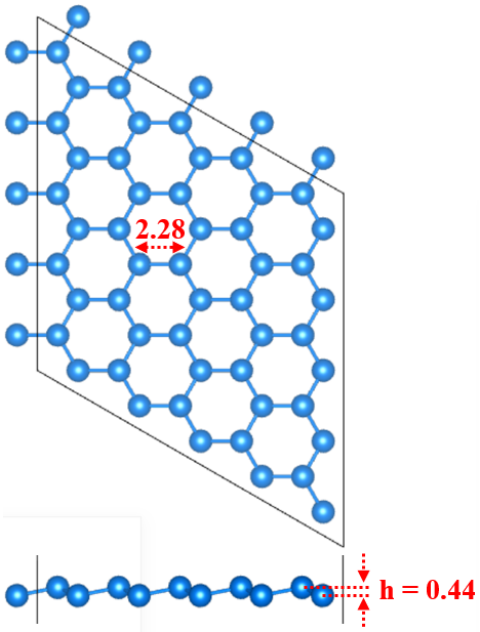

Fig. S1 Schematic representation of pristine Silicene (Si) from both top and side views, together with nearest neighbour distance and buckling height (h). Unit: Å. Color code: Si – light blue.

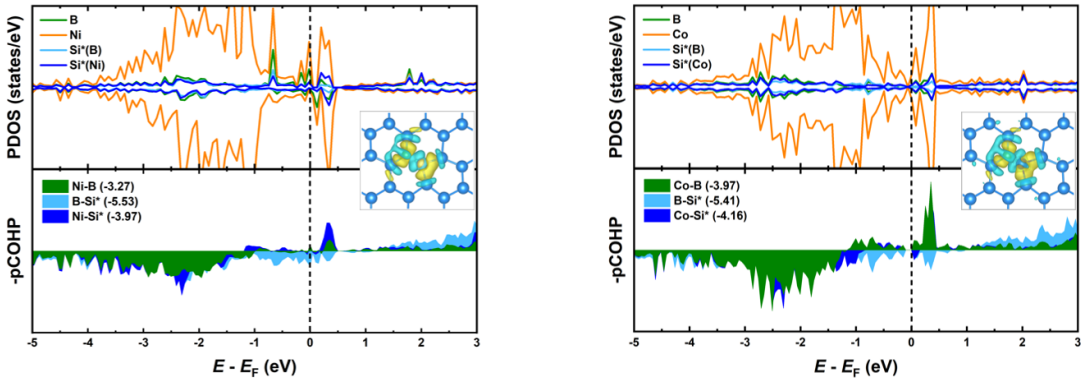

Fig. S2. Partial density of states (PDOS) of dopants (B/Ni/Co) and one their nearest neighboring host atom (Si*); projected crystal orbital Hamilton population (pCOHP) of the dopant-dopant and dopant-host atom bonds within heterogeneous B-Ni@Si and B-Co@Si structures. The Fermi level displayed in dashed line is set to zero. Their corresponding charge density difference are also displayed. The isosurface value is set to 0.0025 e/Å^3, and the yellow (cyan) regions represent charge accumulation (depletion).

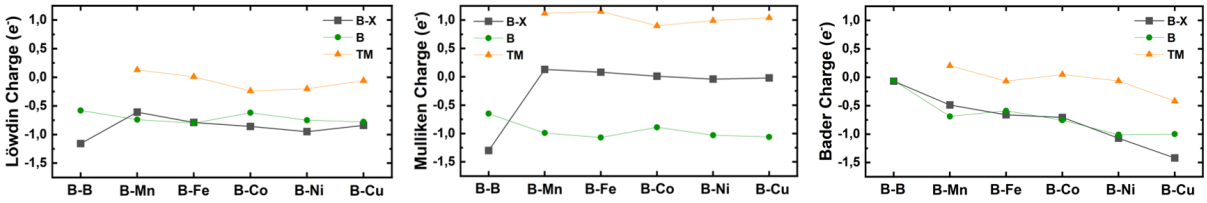

Fig. S3. Löwdin, Mulliken and Bader charge variations of B, transition metals (TM) and total B-X (X: B or TM) pairs within the pure B-X systems.

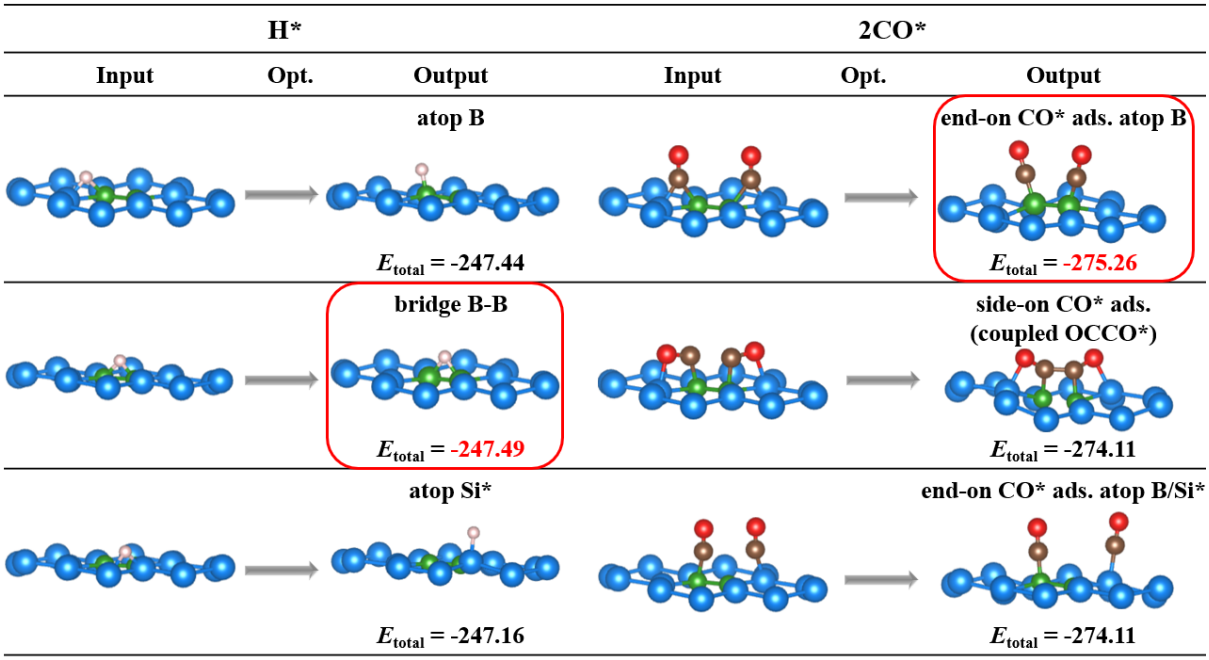

Fig. S4 All possible scenarios of H and 2CO adsorbed on B-B@Si before and after optimization (opt.) with their corresponding total energy (E_{total}). Units: eV. Lowest-energy optimized configurations for the H* and 2CO* intermediates are highlighted in red. Color code: B – green, Si – light blue, H – light pink, C – brown and O – red.

For H* intermediate, regardless of the initial guess of H adsorption sites (atop B, or bridge B-Si*, or Si*-Si*sites, H preferentially absorbs on the bridge site of two dopants (B-B), forming the most stable H* configuration post-optimization. Likewise, for the 2CO* intermediate, the lowest-energy configuration is obtained as two CO molecules vertically adsorb onto two dopant active sites.

Int.	B-B	B-Cu	B-Ni	B-Co
H*	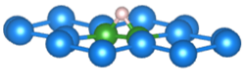		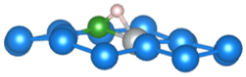	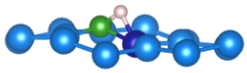
2CO*	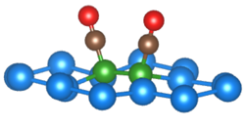	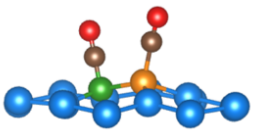	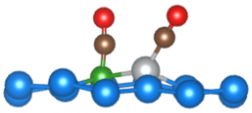	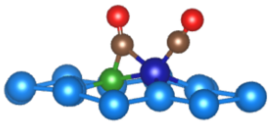

Fig. S5. Corresponding lowest-energy configurations of H* and 2CO* adsorption on B-B@Si, B-Cu@Si, B-Ni@Si and B-Co@Si. Color code: B – green, Co – blue, Ni – silver, Cu – orange, Si – light blue, H – light pink, C – brown and O – red.

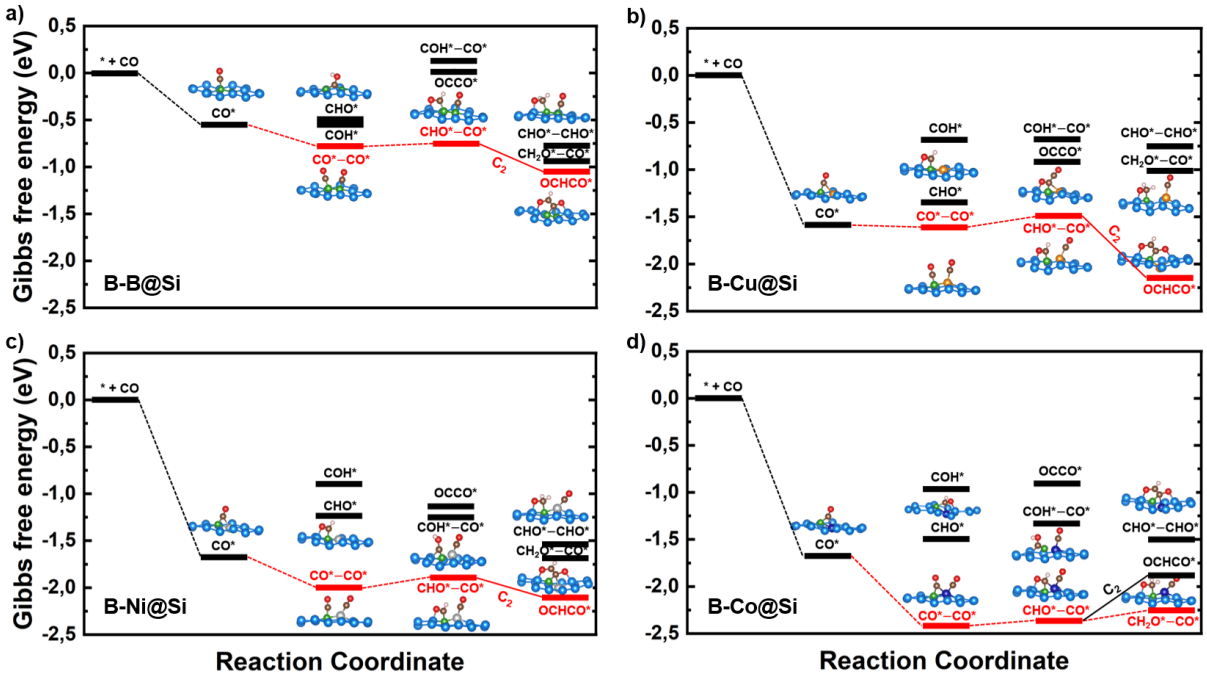

Fig. S6. Free energy profiles possible C_1 and C_2 pathways during the initial stage of CORR process, starting from one CO molecule adsorption on a) B-B@Si, b) B-Cu@Si, c) B-Ni@Si and d) B-Co@Si at 0 V (*vs* RHE). Inserts display the corresponding optimized structures of reaction intermediates. The solid lines indicate the C–C coupling step. The red lines represent the most thermodynamically favorable route. Color code: B – green, Cu – orange, Ni – silver, Co – dark blue, Si – light blue, C – brown, O – red and H – light pink.

Four structures are more energetically inclined to adsorb an additional CO molecule, forming a decoupled CO*−CO* intermediate (comprising two separate C_1 fragments, particularly 2CO*) rather than proceeding with protonation to generate C_1 intermediates (CHO* or COH*). The decoupled CO−CO* intermediate is then more favorably hydrogenated to form decoupled CHO−CO*. The subsequent preferential coupling step of two C_1 fragments (CHO* and CO*) within the decoupled CHO−CO* to form a coupled OCHCO* intermediate occurs on three BACs (B-B@Si, B-Cu@Si and B-Ni@Si), rather than its competitive protonation steps to form decoupled CH_2O*−CO* (or CHO*−CHO*).

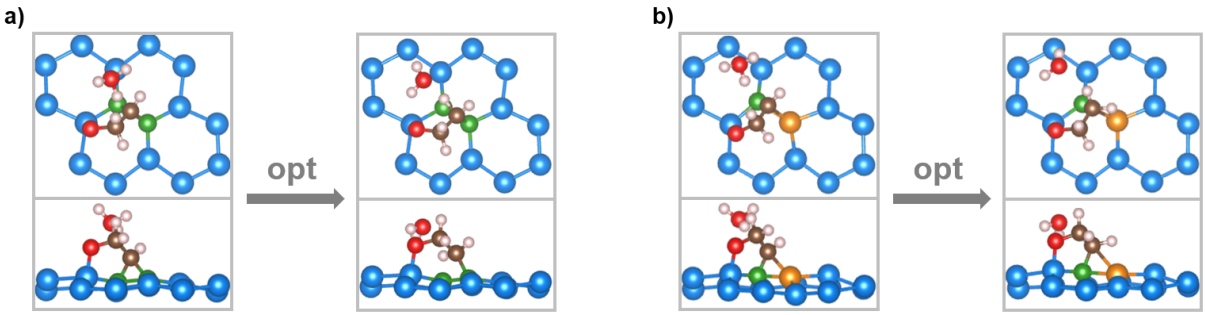

Fig. S7. Top and side views of OCH_2CH^* adsorption on (a) B-B@Si and (b) B-Cu@Si with the presence of H_3O^+ before and after structure optimization. Starting geometries with H_3O^+ placed in the vicinity of OCH_2CH^*.

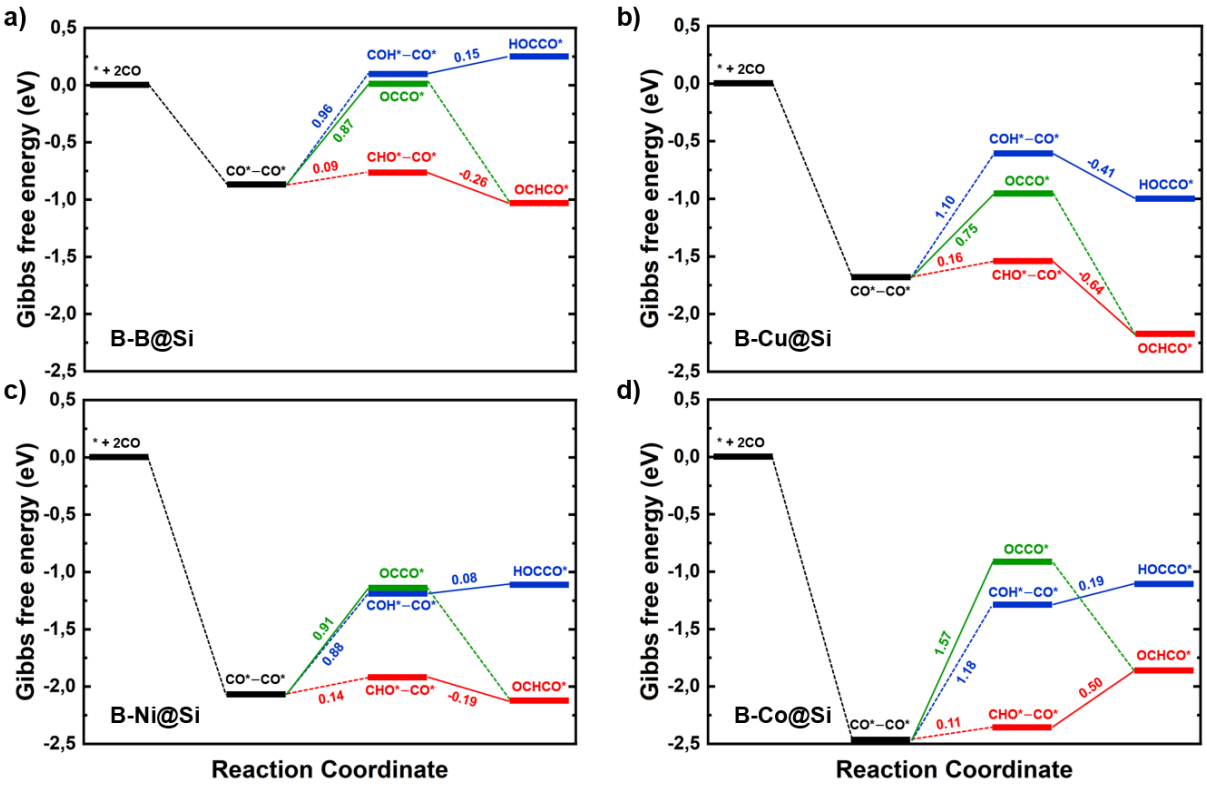

Fig. S8. Free energy profiles of different C-C coupling paths in vacuum on **a)** B-B@Si, **b)** B-Cu@Si, **c)** B-Ni@Si and **d)** B-Co@Si at 0 V (*vs* RHE). The solid lines indicate the C–C coupling step.

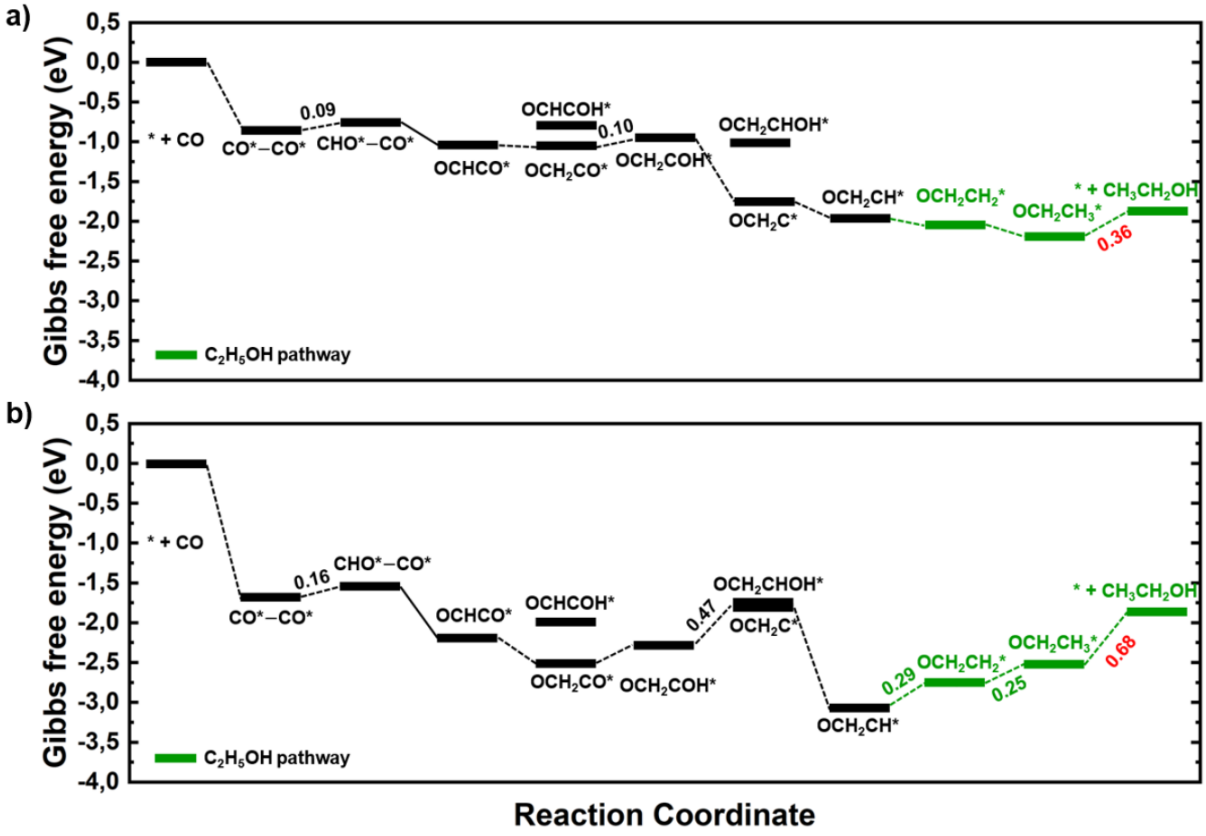

Fig. S9 Free-energy profiles for CO reduction in vacuum on **a)** B-B@Si and **b)** B-Cu@Si. The potential determining step is labeled with the corresponding free energy change in red color. The green line demonstrates the best overall pathways towards CH_3CH_2OH. The solid lines indicate the C–C coupling step.

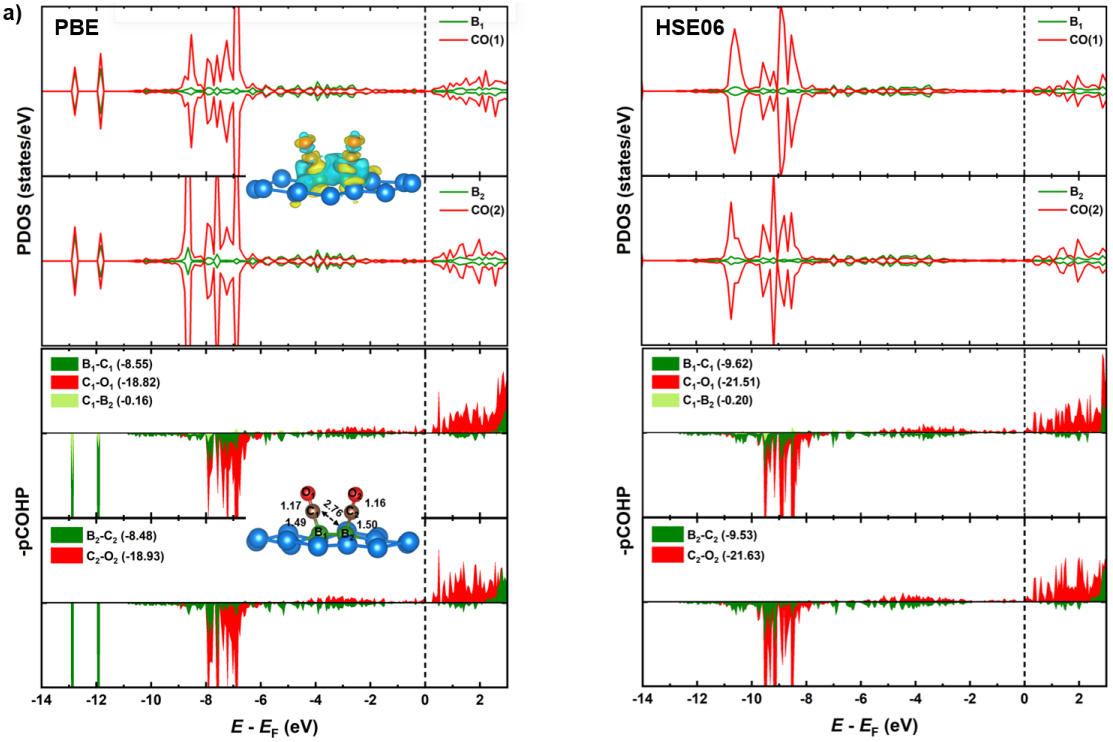
a)
PBE
HSE06
PDOS (states/eV)
B1
CO(1)
B2
CO(2)
B1-C1 (-8.55)
C1-O1 (-18.82)
C1-B2 (-0.16)
B2-C2 (-8.48)
C2-O2 (-18.93)
B1-C1 (-9.62)
C1-O1 (-21.51)
C1-B2 (-0.20)
B2-C2 (-9.53)
C2-O2 (-21.63)
-pCOHP
1.17
2.76
1.16
1.49
1.50
-14 -12 -10 -8 -6 -4 -2 0 2
E - EF (eV)

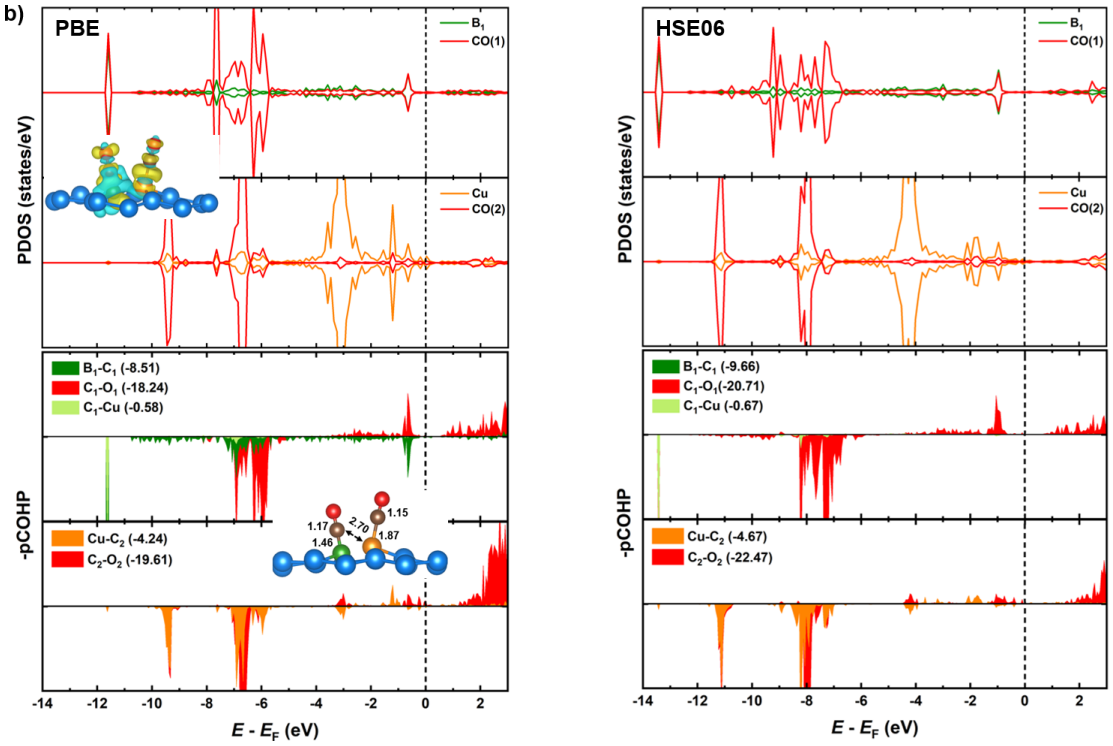
b)
PBE
HSE06
PDOS (states/eV)
B1
CO(1)
Cu
CO(2)
B1-C1 (-8.51)
C1-O1 (-18.24)
C1-Cu (-0.58)
Cu-C2 (-4.24)
C2-O2 (-19.61)
B1-C1 (-9.66)
C1-O1(-20.71)
C1-Cu (-0.67)
Cu-C2 (-4.67)
C2-O2 (-22.47)
-pCOHP
1.17
2.70
1.15
1.46
1.87
-14 -12 -10 -8 -6 -4 -2 0 2
E - EF (eV)

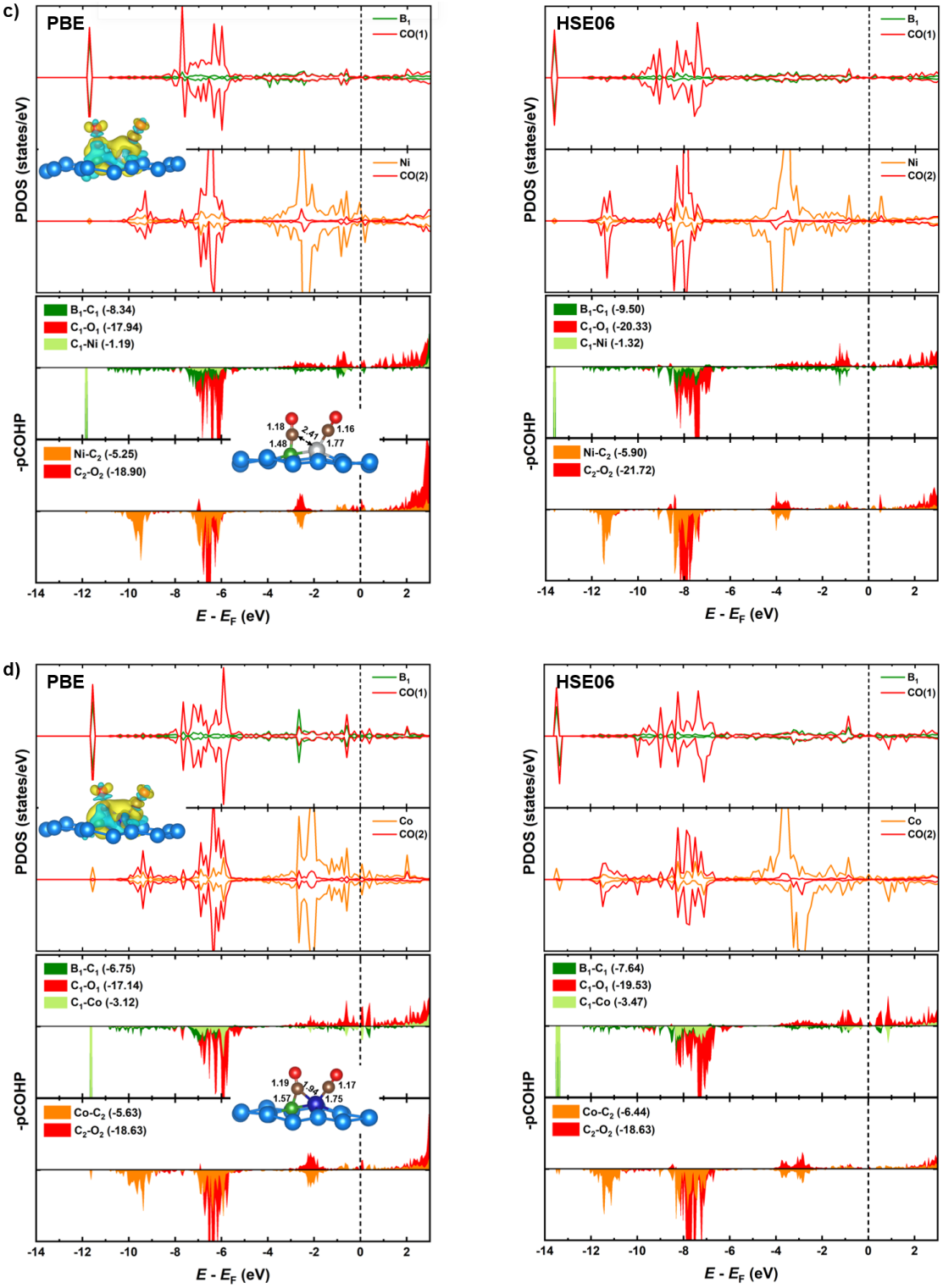

Fig. S10. Partial density of states (PDOS) of dopants and two adsorbed CO* species (upper panels) obtained by PBE and HSE06 functionals on (a) B-B@Si, (b) B-Cu@Si, (c) B-Ni@Si and (d) B-Co@Si. Their corresponding charge density difference are also displayed. The isosurface value is set to 0.0025 e/Å^3, and the yellow (cyan) regions represent charge accumulation (depletion). Projected crystal orbital Hamilton population (pCOHP) of the 2CO* intermediate. The Fermi level displayed in dashed line is set to zero. Their geometries with bond lengths are also displayed.

Systems	d_{B-X} (Å)	d_{B-Si^*} (Å)	d_{TM-Si^*} (Å)
B-B@Si	1.70	2.01	
B-Co@Si	1.91	1.97	2.22
B-Ni@Si	1.96	1.94	2.20
B-Cu@Si	2.02	1.94	2.31

Table S1 Bond lengths of two dopants (d_{B-X}), dopant and its host neighbor (Si*) in B-X@Si. Units: Å

Adsorbed species	IpCOHP (bonds)	Functionals	B-B@Si	B-Cu@Si	B-Ni@Si	B-Co@Si
CO(1)*	C_1-B	PBE	-8.55	-8.51	-8.34	-6.75
		HSE06	-9.62	-9.66	-9.50	-7.64
	C_1-O_1	PBE	-18.82	-18.24	-17.94	-17.14
		HSE06	-21.51	-20.71	-20.33	-19.53
	C_1-B_2(TM)	PBE	-0.16	-0.58	-1.19	-3.12
		HSE06	-0.20	-0.67	-1.32	-3.47
CO(2)*	B_2(TM)-C_2	PBE	-8.48	-4.24	-5.25	-5.63
		HSE06	-9.53	-4.67	-5.90	-6.44
	C_2-O_2	PBE	-18.93	-19.61	-18.90	-18.63
		HSE06	-21.63	-22.47	-21.72	-21.28

Table S2 IpCOHP values of key bonds in CO(1)-CO(2)*-adsorbed B-X@Si intermediates taken from Fig. S10.

Structures	Active sites	Functionals	μ_{CHO-CO^*}	μ_{OCHCO^*}	$\Delta\mu$ (μ_B)
B-B@Si	**B_1**	PBE	0.01	0.00	
		HSE06	0.00	0.00	
	B_2	PBE	0.00	0.00	
		HSE06	0.00	0.00	
	Total (B_1-B_2)	**PBE**	**0.01**	**0.00**	**-0.01**
		HSE06	**0.00**	**0.00**	**0.00**
B-Cu@Si	**B**	PBE	0.00	0.00	
		HSE06	0.00	0.00	
	Cu	PBE	0.00	0.00	
		HSE06	0.00	0.00	
	Total (B-Cu)	**PBE**	**0.00**	**0.00**	**0.00**
		HSE06	**0.00**	**0.00**	**0.00**
B-Ni@Si	**B**	PBE	0.00	0.03	
	Ni	PBE	0.00	0.18	
	Total	**PBE**	**0.00**	**0.21**	**0.21**
B-Co@Si	**B**	PBE	0.00	-0.02	
	Co	PBE	0.00	0.45	
	Total	**PBE**	**0.00**	**0.43**	**0.43**

Table S3 Magnetic moments calculated by PBE and HSE06 functionals in two key intermediates CHO-CO* and OCHCO* intermediates across four systems. Units: μ_B

There is no magnetic moments at the two B active sites in the two CHO-CO*/OCHCO*-adsorbed homo-B-B@Si intermediates, resulting in $\Delta\mu \approx 0\mu_B$. Moreover, the incorporation of Cu in hetero-B-Cu@Si for the two intermediates does not alter their electronic states, also leading to $\Delta\mu = 0\mu_B$. These values, computed using the PBE functional, for the two most promising catalysts, B-B@Si and B-Cu@Si, are also compared with hybrid calculations using the HSE06 functional. Meanwhile, the other two hetero-B-Ni/Co@Si experience a slight change in $\Delta\mu$ ($0.21/0.43\mu_B$), primarily due to the marginally higher spin state of the TM (Ni/Co) in the coupled-OCHCO* intermediate. The importance of spin state is also reflected in the difference in spin-up and spin-down PDOS as shown in Fig. 9.

1 J. K. Nørskov, J. Rossmeisl, A. Logadottir, L. Lindqvist, J. R. Kitchin, T. Bligaard and H. Jónsson, *J. Phys. Chem. B*, 2004, **108**, 17886–17892.
2 J. Greeley and J. K. Nørskov, *Electrochimica Acta*, 2007, **52**, 5829–5836.